Thermodynamic Properties of 5-(4′-isopropylbenzylidene)-2,4-dioxotetrahydro-1,3-thiazole as a Corrosion Inhibitor for Copper in Acid Solution

Gyöngyi Vastag[1,], Jelena Nakomčić[1], Abdul Shaban[2]*

[1] University of Novi Sad, Faculty of Sciences, Department of Chemistry, Biochemistry and Environmental Protection, Trg Dositeja Obradovića 3, 21000 Novi Sad, Serbia
[2] Research Centre for Natural Sciences, Hungarian Academy of Sciences, Magyar tudósok körútja 2, 1117 Budapest, Hungary
[*]E-mail: djendji.vastag@dh.uns.ac.rs

5-(4′-isopropylbenzylidene)-2,4-dioxotetrahydro-1,3-thiazole, (*IPBDT*) was tested as a potential copper corrosion inhibitor in 0.1 mol dm^{-3} Na$_2$SO$_4$ solution at pH=3. Using *dc* polarization measurements and electrochemical impedance spectroscopy (*EIS*) the influence of the inhibitor concentration and temperature on the inhibitor efficiency was investigated. The obtained results suggested that *IPBDT* is a very good copper corrosion inhibitor in given condition, whose efficiency increases with the increase of the thiazole concentration as well as with the increase of temperature. *EIS* results showed that the inhibition effect of the thiazole manifests through an increase of the total resistance and a decrease of the double layer capacitance compared to the blank solution. The kinetic and thermodynamic parameters obtained by the polarization measurements, indicated that the copper corrosion in acidic sulfate solution occurs as an endothermic reaction and that the inhibitor molecules protect the copper during their chemisorption on the metal surface following the Langmuir's adsorption isotherm.

1. INTRODUCTION

In modern industries, copper and its alloys have a very important role in many production processes. Due to its relative nobility, copper corrosion can take place at lower pH values, whereby, the amount of oxygen present in a given environment has a great influence on the degree of copper

corrosion [1,2]. Nowadays an increased interest in the possibility of protecting copper against corrosion using organic inhibitors can be registered. As it is well known, in most cases, efficient copper corrosion inhibitors have nitrogen, sulfur and/or oxygen atoms in their structure [3-6]. Most of them manifest good inhibitory efficiency in neutral media whereas the numbers of molecules which have good inhibition properties in the acid medium are significantly limited [7-12]. The corrosive attack on the metal in acidic media in presence of organic inhibitors will be reduced due to their adsorption on metal surface [13-15]. Adsorption of inhibitor molecules at the metal surface may occur as physisorption or in a better case organic molecules can form covalent bond with metal [16-18]. Modifying functional groups (substituents) into the investigated organic molecules can modulate the interfacial behaviour and inhibitor efficiency of the organic compounds. The group with the most significant impact is the substituting group with electron-donating effect, because it can change electron density of the active center in the molecule. Numerous studies have shown that very often small difference in the molecular structure of corrosion inhibitor can give very different inhibitor efficiency [19-26].

Thiazole derivatives belong to the group of compounds which disposes with the possibility to protect copper in acidic media. The aim of this paper is to study the influence of inhibitor concentration and temperature on the mechanism, kinetic and thermodynamic parameters of copper corrosion processes in the absence and presence of 5-(4′-isopropylbenzylidene)-2,4-dioxotetrahydro-1,3-thiazole (*IPBDT*) using dc polarization measurement and electrochemical impedance spectroscopy, (*EIS*). The result of *dc* polarization measurement provides opportunity to study the corrosion and the inhibitor adsorption mechanism in the function of different inhibitor concentration and temperatures. The *EIS* measurements offer substantial data about kinetic and mechanistic properties of analyzed electrochemical system [27]. It is one of the most commonly used method to assess the protective properties of the inhibitor film formed on metal surface because by using this method, the resistance of charge transfer to the metal surface can be very successfully registered [28]. The *EIS* measurement also can help in prediction of the kinetic properties of electron transfer at the copper/electrolyte interface [29].

2. EXPERIMENTAL

The inhibitor efficiency of 5-(4′-isopropylbenzylidene)-2,4-dioxotetrahydro-1,3-thiazole, *IPBDT* (Figure 1) was investigated on the copper electrode in 0.1mol dm^{-3} Na$_2$SO$_4$ solution at pH=3, against copper corrosion in function of its concentration and temperature.

Because of the low solubility of the investigated inhibitor, the determined weight of the *IPBDT* was first dissolved into 20 ml of ethanol and thereafter solutions of desired concentrations were prepared with distilled water. In each solution, pH was set to 3 with diluted sulfuric acid. All experiments were done at open atmosphere.
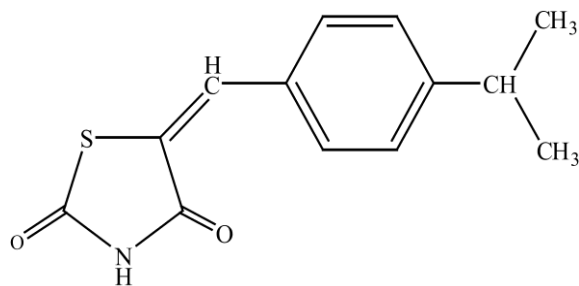
Figure 1. Molecular structure of the investigated inhibitor

The electrochemical measurements were done in the three-electrode cell, copper was the working electrode, the saturated calomel electrode (*SCE*) the reference electrode and the platinum was the counter electrode. The working electrode was constructed from high purity copper rods (99.99 % Cu), watered in an epoxy resin. The active surface of copper electrode (0.7 cm^2) was before each measurement wet polished with SiC papers (grit sizes of 800 and 1200). The electrochemical measurements were carried out with A PC controlled VoltaLab PGZ 301.

The *EIS* measurements were carried out on the open circuit potential, (OCP), at room temperature, after 30 minutes of immersion time of electrode in the solution with different *IPBDT* concentrations (1x10^{-6}- 1x10^{-5} mol dm^{-3}). The *EIS* working conditions were 10 mV amplitude of sinusoidal voltage in a frequency range of 0.01Hz-10 KHz. The impedance spectra were analyzed using the program *Eissa_0.1b*.

The polarization measurements were performed also at five different inhibitor concentrations in the range of 1x10^{-6}- 1x10^{-5} mol dm^{-3}, at four temperatures 288, 293, 303 and 308 K. The potential was scanned between OCP and 400 mV in the cathodic and OCP and 200 mV to anodic directions with the scan rate of 10 mV min^{-1} after the open circuit potential was stabilized to 5 mV/5 min.

3. RESULTS AND DISCUSSION

3.1. EIS results

As is well known, the dissolution of copper in aerated sulfuric acid includes two reactions: the anodic dissolution of copper and the cathodic reduction of oxygen. The anodic reaction takes place in two continuous steps:

$$Cu \rightarrow Cu^+_{ads} + e^- \tag{1}$$
$$Cu^+_{ads} \rightarrow Cu^{2+} + e^- \tag{2}$$

where Cu^+_{ads} is an adsorbed species at the copper surface, which does not exhibit a tendency for diffusion into the solution [30-33]. Because of this, the copper dissolution usually just weakly depends of the mass transport. The size and shape of *EIS* spectra can be changed (e.g, increase of the capacitive loop) with the extension of the immersion time, which can be considered as an indication that some kind of barrier formed on the metal surface. The barrier is probably related to the formation of the salt film of copper ions. Cu_2O and CuO cannot exist in strong acidic solutions [34].

Cathodic reduction of oxygen can be described either by a direct 4e- transfer:

$$O_2 + 4H^+ + 4e^- \rightarrow 2H_2O \tag{3}$$

or by two consecutive 2e- steps which include first a reduction to hydrogen peroxide:

$$O_2 + 2H^+ + 2e^- \rightarrow 2H_2O_2 \tag{4}$$

which was followed by a second reduction [34,35]:

$$H_2O_2 + 2H^+ + 2e^- \rightarrow 2H_2O \tag{5}$$

Regardless of whether the reduction of oxygen takes place in one or two steps, the decisive influence on the rate of cathodic oxygen reduction have oxygen transfer from the bulk solution to the Cu-solution interface [34].

To better understand the mechanism of the interaction between the copper surface and the investigated inhibitor molecules in acidic sulfate solutions, an *EIS* measurement was carried out in the presence of different concentration of *IPBDT* in a range of 1×10^{-6}- 1×10^{-5} moldm^{-3} at room temperature.

Figures 2a and 2b depict the Nyquist plots for copper the electrode in 0.1 moldm^{-3} Na$_2$SO$_4$ solution without and with the addition of different concentration of inhibitor respectively.
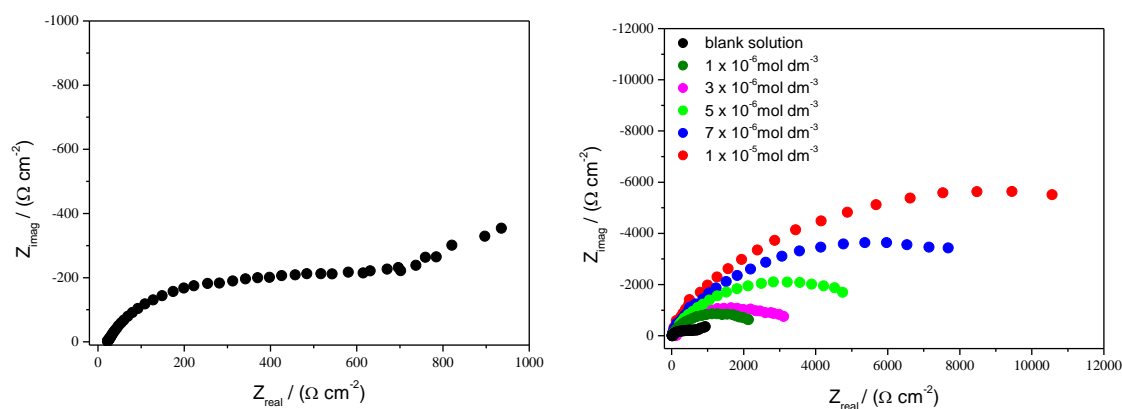

Figure 2. Nyquist dijagram for copper in blank solution (a) and in the presence of different concentration of *IPBDT* (b)

As Figures 2a and 2b show, in all cases the not perfect semicircles were obtained, which is characteristic for copper in acidic sulfate solution [30,36]. This phenomena is often attributed to the dispersion of frequency, heterogeneity of the metal surface and/or the inhibitor adsorption [37-42].

The impedance spectra recorded in blank solution consists of two parts: at the higher frequencies range, a single semicircle capacitive loop was recorded which is followed by the Warburg impedance in the low frequencies. The high frequency capacitive loop, describe the charge transfer resistance together with the double-layer capacitance element [43], while the Warburg impedance is mainly referred to diffusion of the oxygen from solution to the copper surface [44].

The presence of the thiazole derivative in the acidic sulfate solution did not lead to significant shifts of copper corrosion potentials compared to the bare electrode, but led to changes in the shape and size of the impedance spectra. In the presence of the thiazole derivative in the high frequency

region a larger capacitive loop can be registered and the Warburg impedance also disappears. This kind of behaviour indicated that the *IPBDT* molecule can form a film on the metal surface and protect the copper against corrosion [45]. Increasing inhibitor concentrations also leads to the increase of the capacitive loop, which provides better protection of the copper in the presence of higher inhibitor concentrations [46] and on the other hand indicated that the charge transfer resistance becomes dominant in the corrosion process [4].

The experimentally recorded *EIS* results were fitted with the equivalent circuit using the *Eissa_0.1b* program and obtained models are presented in Figure 3a for corrosion solution and Figure 3b for inhibitor solutions.
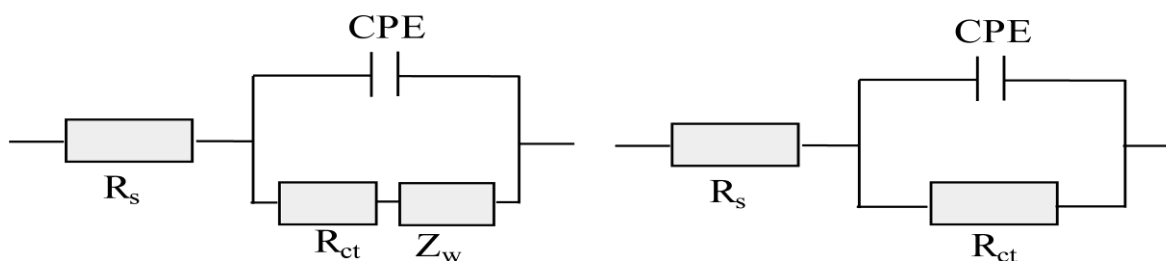

Figure 3. Electrical equivalent circuit for Cu electrode in 0.1 mol dm^{-3} Na$_2$SO$_4$ without (a) and with the addition of *IPBDT* (b).

In the equivalent circuits, R_s is the solution resistance, Rc_t the charge-transfer resistance, Z_w Warburg impedance and *CPE* represent the double-layer constant phase elements.

When there is an unideal semicircle in the EIS result, a *CPE* is usually used for a better fit instead. The impedance of a *CPE* is given by

$$Z_{CPE} = \frac{1}{Y_0}(j\omega)^{-n} \tag{6}$$

where is; Y_0 the magnitude of *CPE* and ω the angular frequency and n the exponential term of the *CPE* ($0 \leq n \leq 1$) [47-48].

The value of n indicates the distribution of time constants caused by the electrode surface roughness or inhomogeneities in the inhibitor film formed on the copper surface [49]. The smaller value of n means the higher surface roughness of the electrode [43-44]. Value of n also may indicate the depressed feature of the impedance spectra. Values closer or lower than 0.5 indicates that the diffusion process may take place, if n is considerably higher than this values (as in the presence of *IPBDT*), semicircular obtained in *EIS* measurement describing the reduction-oxidation process including corrosion products and/or dissolved oxygen [24].

Hsu and Mansfeld formula [50-51], which is widely used to extract effective capacitance values from the *CPE* parameter in case of corrosion inhibitors [52] was also used in our investigation.

Table 1 presents the result obtained by fitting the *EIS* results, open circuit potential of copper electrodes (*E*), and inhibition efficiency (*η*), which was calculated using the following equation:

$$\eta\ (\%)\ = \frac{R_{ct} - R_{ct}^0}{R_{ct}} \cdot 100 \tag{7}$$

In which R_{ct}^0 and R_{ct} represent the charge transfer resistance in the absence and presence of the inhibitor, respectively.

Table 1. Impedance parameters and inhibition efficiency of *IPBDT*

c_{inh} / (mol dm^{-3})	E / mV	R_{ct} / Ω	C_{dl}/ (mF cm^{-2})	n	η / %
0	-57	620	15.75	0.67	/
1x10^{-6}	-52	2600	15.00	0.75	76
3x10^{-6}	-49	3350	12.38	0.74	82
5x10^{-6}	-40	6300	9.21	0.75	90
7x10^{-6}	-30	10700	7.25	0.76	94
1x10^{-5}	-23	16250	4.40	0.77	96

*Warburg impedance in the blank solution was 13 Ω

Results in Table 1 show that the presence of thiazole derivative in acidic sulfate solution, did not lead to significant shifts of copper corrosion potentials compared to the bare electrode. The inhibition effect of *IPBDT* on copper corrosion in acidic solution is reflected by increases of the charge transfer resistance, R_{ct} and in decrease of the double layer capacitance, C_{dl} related to the blank solution. The increase of charge transfer resistance present is evidence of the protective film formation on the copper surface which can block the dissolution of the metal in this condition [53,11]. The decrease of the double layer capacitance in the presence of inhibitor compared to the blank solutions can be explained by the displacement of the water molecules and ions from the double-layer by the neutral inhibitor molecules. Since the organic molecules manly have a much lower value of dielectric constant than water, replacing the water molecules with inhibitors leads to lower values of the double layer capacitance.

3.2. Potentiostatic Polarization Measurements

3.2.1. Effect of inhibitor concentration

The obtained polarization curves of the copper electrode in 0.1 mol dm^{-3} Na$_2$SO$_4$ solutions with and without addition of different concentrations of *IPBDT* at 293K are shown in Figure 4

The corrosion current density (*j*) values were obtained through Tafel plots, by extrapolation of the linear cathodic and anodic Tafel regions on the corrosion potential, *E*.

Using the obtained corrosion current densities the corrosion inhibition efficiency, η, can be calculated using the following equation:

$$\eta \ (\%) \ = \ 1 \ - \ \frac{j}{j_0} \cdot 100 \qquad (8)$$

where, j_0 and j represent the corrosion current density in the absence and presence of the inhibitor, respectively.

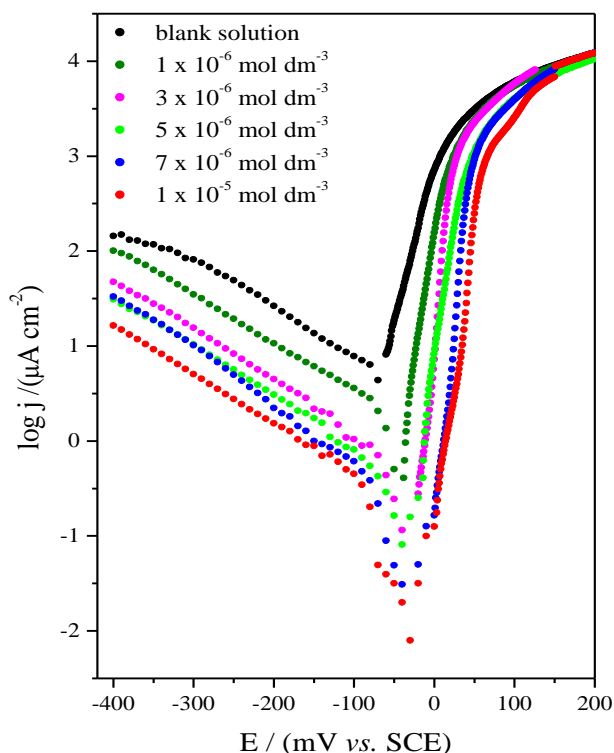The obtained results in all temperatures are given in Table 2.

Figure 4. Polarization curve for copper in blank solution and in presence of different concentration of *IPBDT* at 293 K

The results in Table 2 show that the presence of the inhibitor in the solution at any concentration and any temperature does not cause a significant shift of the corrosion potential towards the anode or cathode side compared to the blank solution. It is means that the inhibitor acted by merely blocking the reaction sites of the metal surfaces without changing the reaction mechanisms [54] and also indicates that the *IPBDT* might act as a mixed-type inhibitor [11].

The data in Table 2 also shows that presence of *IPBDT* leads to significant reduction of corrosion current densities, increasing of inhibitor concentration has the same effect. Consequently, the inhibition efficiency of *IPBDT* is increasing in a function of its concentration.

The high inhibitor efficiency of *IPBDT* derivative may be explained by the presence of the isopropyl group in the molecule. The isopropyl group is powerful electron-donors due to its positive inductive and resonance effects, accompanied by hyperconjugation. Thanks to these effects, the electron density of the active center of thiazole molecules is increasing, due to which a stronger interaction (bonds) can be achieved between the copper and *IPBDT* molecules [13].

Table 2. Parameters of polarization measurements and inhibition efficiency in different concentration of *IPBDT* and at different temperature

c_{inh} / (mol dm^{-3})	T / K	E / mV	j / (μA cm^{-2})	η / %	θ
	288				
0		-62	2.100	-	-
1x10^{-6}		-49	1.259	40.0	0.400
3x10^{-6}		-44	0.393	81.3	0.813
5x10^{-6}		-40	0.294	86.0	0.860
7x10^{-6}		-41	0.235	88.8	0.888
1x10^{-5}		-13	0.175	91.7	0.917
	293				
0		-51	4.320	-	-
1x10^{-6}		-36	1.371	68.3	0.683
3x10^{-6}		-49	0.421	90.3	0.903
5x10^{-6}		-20	0.312	92.8	0.928
7x10^{-6}		-37	0.250	94.2	0.942
1x10^{-5}		-33	0.179	95.9	0.959
	303				
0		-57	37.42	-	-
1x10^{-6}		-50	1.609	95.7	0.957
3x10^{-6}		-43	0.485	98.7	0.987
5x10^{-6}		-37	0.355	99.1	0.991
7x10^{-6}		-19	0.279	99.2	0.992
1x10^{-5}		-10	0.187	99.4	0.994
	308				
0		-55	93.50	-	-
1x10^{-6}		-47	1.748	98.1	0.981
3x10^{-6}		-39	0.536	99.4	0.994
5x10^{-6}		-39	0.393	99.6	0.996
7x10^{-6}		-9	0.294	99.7	0.997
1x10^{-5}		-5	0.191	99.8	0.998

3.2.2 Effect of temperature

Insight into the influence of temperature on the inhibitor efficiency as well as into the corrosion activation energies in the blank and also in the inhibitor solution, offers the possibility of predictions the potential inhibitor adsorption mechanism [55].

As data presented in Table 2 indicates, increasing the temperature causes the increase of corrosion current densities compared to the solution with the same inhibitor concentration at a lower temperature. What is also obvious is that increasing the temperature results in a much larger increase in the corrosivity of the blank solution. The final result of these effects is that in all inhibitor solutions the increase in temperature resulting in an increase of the inhibitor efficiency. The fact that inhibitor efficiency depends on temperature can be explained by the specific interaction between organic compounds and metal surface [56] or as changing the adsorption nature [56-58]. From the result in

Table 2 it is evident that the inhibitor efficiency of *IPBDT* derivative is much more dependent on the applied concentration than on the temperature.

The influence of the temperature on the corrosion rate may be described by using the Arrhenius-type plot and transition state according to the following equation:

$$j = A \exp\left(-\frac{E_a}{RT}\right) \tag{9}$$

Where j is corrosion current density, A is the Arrhenius constant, T is the absolute temperature, R is the universal gas constant and E_a is the activation energy of corrosion reaction.

The E_a values were calculated in the blank and in the *IPBDT* solutions from the slop of $\ln j$ versus 1/T plots (Figure 5). Obtained results are shown in Table 3.
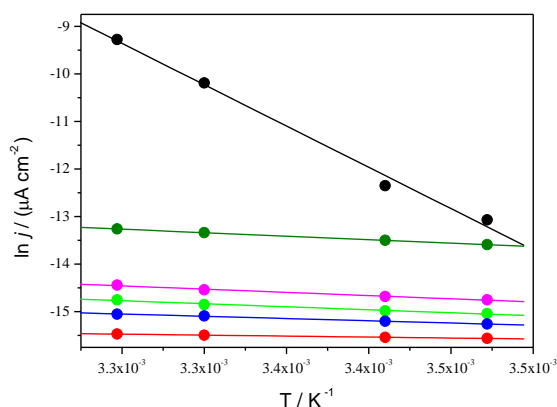

Figure 5. Arrhenius plots for copper corrosion in the blank and in the *IPBDT* solutions

Table 3. Kinetic parameters for copper corrosion at different concentrations of *IPBDT*

c_{inh} / (mol dm^{-3})	$\ln A$	E_a / (kJ mol^{-1})	R	ΔH_a° / (kJ mol^{-1})	ΔS_a° / (J mol^{-1} K^{-1})	R
0	47.05	144.32	0.996	141.85	138.00	0.996
1×10^{-6}	-8.51	12.17	0.999	9.62	-324.20	0.999
3×10^{-6}	-10.05	11.26	0.996	9.02	-336.77	0.993
5×10^{-6}	-10.66	10.51	0.993	8.03	-341.85	0.987
7×10^{-6}	-11.97	7.87	0.999	5.79	-351.41	0.999
1×10^{-5}	-14.16	3.35	0.999	0.74	-371.39	0.999

As the result in Table 3 indicates, the presence of thiazole derivative causes the significant decrease in the activation energy, which is further decreased with the increase of *IPBDT* concentration. This type of behavior is typical for chemisorptions [59-60].

The Arrhenius constant behaves very similarly to the activation energy, decreasing with the increase of inhibitor concentration. In the present study, the decrease in corrosion current densities can be determined by the decrease of the Arrhenius constant.

Using the transition-state equation:

$$j = \frac{RT}{Nh}\exp\left(-\frac{\Delta S_a^0}{R}\right)\exp\left(-\frac{\Delta H_a^0}{RT}\right) \qquad (10)$$

enthalpy of activation (ΔH_a^o) and the entropy of activation (ΔS_a^o) were determined.

Where j is the corrosion current density, T is the absolute temperature, R is the universal gas constant, h is Plank's constant, N is Avogadro's number, ΔS_a^o is the activation entropy and ΔH_a^o is the activation enthalpy. The straight lines obtained in correlation ln (j/T) against 1/T, with a slope ($-\Delta H_a^o/R$) and an intercept of [(ln (R/Nh)) + ($\Delta S_a^o/R$)] were used for calculation. Transition state plots for copper corrosion in the blank and in the *IPBDT* solutions are shown in Figure 6.
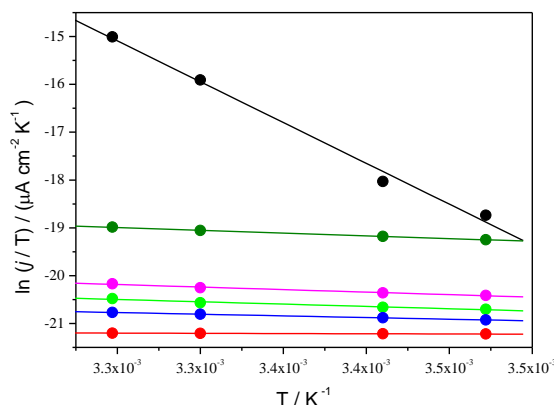

Figure 6. Transition-state plots for copper corrosion in the blank and in the *IPBDT* solutions

The determined kinetic parameters for copper corrosion in 0.1 mol dm^{-3} Na$_2$SO$_4$ solution (pH 3) without and with various concentrations of *IPBDT* are listed in Table 3.

As results presented in Table 3 show the activation enthalpy, ΔH_a^o has positive value in all solution, which noticeably decreases with the presence of *IPBDT* in solution and significantly smaller decreases with the increase of the inhibitor concentration. The positive value of ΔH_a^o indicates that the dissolution of copper in given condition is endothermic process, which also represents a sign that the copper corrosion in inhibitor solution is slow [61].

The negative value of ΔS_a^o in all inhibitor solution (Table 3) is a sign that in the opposite of a blank solution during the activation complex formation from reactants a decrease in the disordering takes place. This means that the activation complex formation represent an association rather than a dissociation step [58, 62-63].

As already previously mentioned, the corrosive attack on the metal in acidic media in the presence of investigated thiazole derivatives will be reduced due to their adsorption on the copper/solution interface. During the adsorption at metal surface, inhibitor molecules can successively replace the already present water molecules [64]:

$$inh_{(sol)} + nH_2O_{(ads)} \rightarrow inh_{(ads)} + nH_2O \qquad (11)$$
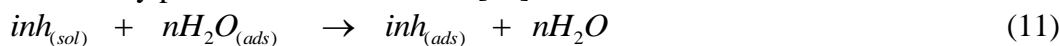
Where *n* is the number of water molecules which can be substituted with one inhibitor molecule.

Important information about the nature of the interaction between the inhibitor molecules and the metal surface as well as between the adsorbed inhibitor molecules themselves can be obtained using adsorption isotherm [65].

The value of the degree of surface coverage, θ, were calculated from following equation:

$$\theta = 1 - \frac{j}{j_0} \tag{12}$$

corresponding to different concentration of the investigated thiazole derivatives at 288, 293, 303 and 308 K were used to found isotherm which with sufficient reliability describes the adsorption process (Table2). The best coincidence between the experimental results and the adsorption isotherms in the studied temperature range was obtained using the Langmuir adsorption isotherm:

$$\frac{c_{inh}}{\theta} = \frac{1}{K_{ads}} + c_{inh} \tag{13}$$

where θ is the surface coverage, c_{inh} is the inhibitor concentration and K_{ads} is the constant of the adsorption process.

The plot c_{inh}/θ against c_{inh} using equation 13, gave a straight line (Figure 7), whose intercept defines the constant of the adsorption process K_{ads}.
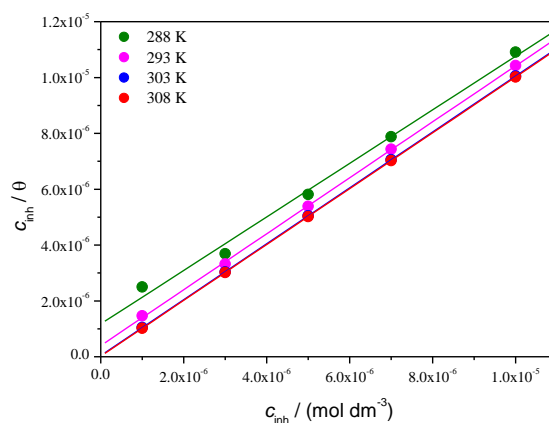

Figure 7. Langmuir's adsorption isotherm of *IPBDT* on the copper surface at different temperatures

The constant of the adsorption process K_{ads}, obtained from the isotherms was used to determine the standard free energy of the adsorption (ΔG_{ads}^{o}) according to the equation:

$$K_{ads} = \frac{1}{55.5} e^{-\left(\Delta G_{ads}^{0}/RT\right)} \tag{14}$$

where 55.5 corresponds to the water concentration in mol dm^{-3}.

Through the thermodynamic basic equation:

$$\Delta G_{ads}^{0} = \Delta H_{ads}^{0} - T\Delta S_{ads}^{0} \tag{15}$$

standard free energy of the adsorption is in connection with the standard enthalpy (ΔH_{ads}^{o}) and standard entropy of the adsorption process (ΔS_{ads}^{o}). Figure 8 shows ΔG_{ads}^{o} values in a function of temperature. The obtained straight line is defined with ΔH_{ads}^{o} as intercept and ΔS_{ads}^{o} as slopes.
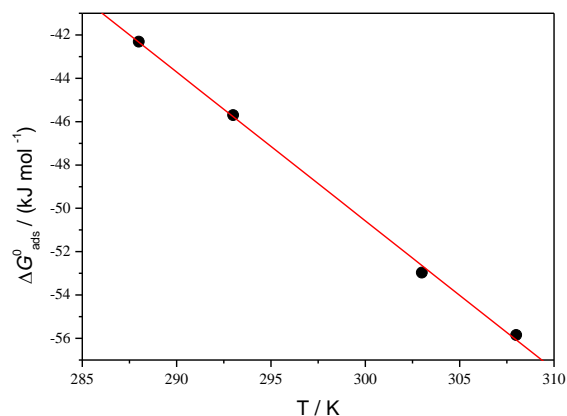

Figure 8. Variation of ΔG_{ads}^{o} in a function of temperatures

Table 4 reports the data from the Langmuir adsorption isotherm and the value of ΔG_{ads}^{o} ΔH_{ads}^{o} and ΔS_{ads}^{o}. As values of the slope and regression coefficient, *R* shown in the Table 4 confirms, the Langmuir adsorption isotherm can describe well the adsorption of *IPBDT* on the copper surface in given conditions. For molecules whose adsorption follows the Langmuir adsorption isotherm is characteristic chemisorption in monolayer [58].

Table 4. The adsorption characteristics of *IPBDT* on the copper surface in acidic sulfate solution

Temp K	Slope	R	ln K_{ads} dm^3 mol^{-1}	ΔG_{ads}^{o} kJ mol^{-1}	ΔH_{ads}^{o} kJ mol^{-1}	ΔS_{ads}^{o} J mol^{-1} K^{-1}
288	0.959	0.997	13.65	-42.31		
293	1.002	0.999	14.74	-45.70	155.47	686.82
303	1.001	0.999	17.01	-52.97		
308	1.001	0.999	17.79	-55.85		

The constant of the adsorption process, K_{ads}, has a relatively high value in all temperatures. This fact suggests that the investigated tiazole derivative, at least in short time, was adsorbed on the metal surface. In the higher temperature, value of K_{ads} increases, this behaviour indicates that the adsorption processes of *IPBDT* on the copper surface becomes faster.

The negative values of ΔG_{ads}^{o} (Table 4) point to a spontaneous adsorption of the thiazole derivative on the copper surface in acidic Na$_2$SO$_4$ solution and stability of the obtained inhibitor layer. Generally, values of ΔG_{ads}^{o} can indicate the type of adsorption. Research has shown that adsorption of

the inhibitor molecules at the metal surface occur as physisorption if the value of ΔG_{ads}^{o} is around -20 kJ mol^{-1} or less, while values around -40 kJ mol^{-1} or more negative suggest that the adsorbed organic molecules can form a coordinate covalent bond with metal (chemisorptions) [66-67]. The calculated ΔG_{ads}^{o} values (Table 4) indicated that in the case of *IPBDT*, the chemisorption of the inhibitor molecules occurs in all temperature ranges. This means that the unshared electron pairs on hetero atoms may interact with the copper d-orbitals to provide a chemisorbed inhibitor film [13, 68-69]. The high electron density around the active center of the molecule which is enough to form a chemical bond with the copper occurs as a result of positive inductive, positive resonance effects, and hyperconjugation effect of isopropyl group. The increase of temperature leads to the increase of ΔG_{ads}^{o} values.

The obtained thermodynamic parameters for the adsorption processes of *IPBDT* at copper surface are important because can point to the inhibition mechanism. Positive values of the heat of adsorption ΔH_{ads}^{o} indicated an endothermic adsorption process which is definitely characteristic of chemisorptions [65, 70] and negative values of this parameter is characteristic to exothermic adsorption which may involve both adsorption types. In the case of *IPBDT* positive values of the heat of adsorption ΔH_{ads}^{o} was obtained (Table 4), which confirms the expected behaviours of *IPBDT*.

Table 4 also shows that the ΔS_{ads}^{o} in presence of *IPBDT* has large and positive values. Because adsorption of inhibitor molecules on the metal surface involves successive desorption of water molecules [10, 71], the obtained values of ΔS_{ads}^{o} are complex and represents the algebraic sum of these two processes. The positive sign of the ΔS_{ads}^{o} values indicated that during the adsorption of *IPBDT* molecules at copper surface, an increase in disordering takes place [58], which at the same time represents the driving force for the inhibitor adsorption [72]. The increase in the solvent entropy and more positive water desorption entropy may also be the reason for the positive values of ΔS_{ads}^{o} [73].

The integrated version of van't Hoff equation expressed by:

$$\ln K_{ads} = -\frac{\Delta H_{ads}^{0}}{RT} + const \qquad (16)$$

also offers the possibility of calculating ΔH_{ads}^{o} and ΔS_{ads}^{o}. Plot ln K_{ads} versus 1/ T gives a straight line (Figure 9), whose slope is equal to $-\Delta H_{ads}^{o}/R$ and intercept to $\Delta S_{ads}^{o}/R + ln$ 1/55.5

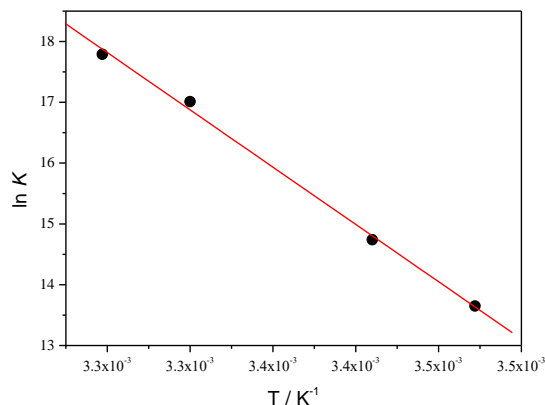**Figure 9.** Van't Hoff plots for *IPBDT* on the copper surface

Calculated ΔH_{ads}^{o} value of 156.65 kJ mol^{-1} and ΔS_{ads}^{o} of 690.67 J mol^{-1} K^{-1} are very similar to values which were obtained by using the thermodynamic basic equation (Table 4).

4. CONCLUSIONS

The fundamental kinetic and thermodynamic parameters for copper corrosion in acidic Na$_2$SO$_4$ solution (pH 3) was determined in basis solution and in the presence of 5-(4′-isopropylbenzylidene)-2,4-dioxotetrahydro-1,3-thiazole, *IPBDT*. The obtained result indicated that the copper corrosion in 0.1 mol dm^{-3} acidic Na$_2$SO$_4$ solution at pH=3 occurs as an endothermic reaction and also confirmed that the *IPBDT* molecules protect the copper surface during their endothermic chemisorption on the metal surface following the Langmuir's adsorption isotherm. *IPBDT* acts as a mixed inhibitor against the cooper corrosion in the given condition. Inhibition efficiency of the investigated thiazole is very good due to the presence of the isopropyl group and it increases with the increase of the thiazole concentrations as well as with the increase of temperature. The protecting effect of the investigated thiazole derivative against copper corrosion in *EIS* results are manifested in the form of an increase of the total resistance and a decrease of the double layer capacitance compared with the blank solution.

References

1. R. Otasuka, M. Uda, *Corros. Sci.*, 9 (1969) 703.
2. A. H. Moreira, A. V. Benedetti, P. L. Calot, P. T. A. Sumodjo, *Electrochim. Acta,* 38 (1993) 981.
3. M. M. Antonijevic, M. B. Petrovic, *Int. J. Electrochem. Sci.,* 3 (2008) 1.
4. M. Behpour, N. Mohammadi, *Corros. Sci.*, 65 (2012) 331.
5. L. Hu, S. Zhang, W. Li, B. Hou, *Corros. Sci.,* 52 (2010) 2891.
6. M. B. Petrovic, M. M. Antonijevic, *Int. J. Electrochem. Sci.,* 10 (2015) 1027.
7. G. Moretti, F. Guidi, *Corros. Sci.*, 44 (2002) 1995.
8. A. Soumoue, B. El Ibrahimi, S. El Issami, L. Bazzi, *International Journal of Science and Research*, 3 (2014) 349.
9. M. Bozorg, T. S. Farahani, J. Neshati, Z. Chaghazardi, G. M. Ziarani, *Ind. Eng. Chem. Res.* 53 (2014) 4295.
10. A. Zarrouk, B. Hammouti, A. Dafali, F. Bentiss, *Ind. Eng. Chem. Res.* 52 (2013) 2560.
11. Z. Tao, W. He, S. Wang, G. Zhou, *Ind. Eng. Chem. Res.* 52 (2013) 17891.
12. A. T. Simunović, M. B. Petrović, M. B. Radovanović, S. M. Milić, M. M. Antonijević, *Chem. Pap.,* 68 (2014) 362.
13. Gy. Vastag, E. Szőcs, A. Shaban, I. Bertóti, K. Popov-Pergal, E. Kálmán, *Solid State Ionics* 141 (2001) 87.
14. Gy. Vastag, E. Szőcs, A. Shaban, E. Kálmán, *Pure Appl. Chem.,* 73 (2001) 1861.
15. Dj. Vaštag, S. Apostolov, M. Hadžistević, M. Sekulić, *Mater. Tehnol.*, 47 (2013) 329.
16. H. Luo, Y. C. Guan, K. N. Han, *Corrosion,* 54 (1998) 619.

17. G. Trabanelli, *Corrosion Mechanism*, Marcel Dekker Inc, (1987) New York, USA
18. Z. Z. Tasic, M. M. Antonijevic , *Chem. Pap.,* 70 (2016) 620.
19. H. Otmacic, E. Stupnisek-Lisac, *Electrochim. Acta,* 48 (2003) 985.
20. A.Shaban, Gy.Vastag, L.Nyikos, *Int. J. Corros. Scale Inhib.*, 4 (2015) 328.
21. Y. Tan, M. Srinivasan, S. Pehkonen, S. Chooi, *Corros. Sci.*, 48 (2006) 840.
22. K. Khaled, N. Heckerman, *Electrochim. Acta,* 49 (2004) 485.
23. M. Scendo, *Corros. Sci.*, 49 (2007) 2985.
24. H. O. Curkovic, E. Stupnisek-Lisac, H. Takenouti, *Corros. Sci.*, 51 (2009) 2342.
25. I.H.R.Tomi, A.H.R.Al-Daraji, S.A.Aziz, *Synthesis and Reactivity in Inorganic, Metal-Organic, and Nano-Metal Chemistry*, 45 (2015) 605.
26. J. Nakomčić, Gy. Vastag, A. Shaban, L. Nyikos, *Int. J. Electrochem. Sci.,* 10 (2015) 5365.
27. E. M. Sherif, R. M. Erasmus, J. D. Comins, *J. Colloid Interf. Sci.,* 311 (2007) 144.
28. E. Abelev, D. Starosvetsky, Y. Ein-Eli, *Langmuir,* 23 (2007) 11281.
29. E. S. M. Sherif, S. M. Park, *Electrochim. Acta,* 51 (2006) 4665.
30. D. K. Y. Wong, B. A. Coller, D. R. WMacFarlane, *Electrochim. Acta,* 38 (1993) 2121.
31. W. H. Smyrl, *Comprehensive Treatise of Electrochemistry*, (1981) Plenum Press, New York, USA
32. E. Mattsson, J. M. Bockris, *Trans. Faraday Soc.*, 55 (1959) 1586.
33. T. Hurlen, G. Ottesen, A. Staurset, *Electrochim. Acta*, 23 (1978) 39.
34. H. Ma, S. Chen, B. Yin, S. Zhao, X. Liu, *Corros. Sci.*, 45 (2003) 867.
35. P. Jinturkar, Y. C. Guan, K. N. Han, *Corrosion,* 54 (1984) 106.
36. Y. Feng, K. S. Siow, W. K. Teo, K. L. Tan, A. K. Hsieh, *Corrosion,* 53 (1997) 389.
37. F. de Souza, R. Gonçalves, A. Spinelli, *J. Braz. Chem. Soc., 25* (2014) 81.
38. S. K. Shukla, M. A. Quraishi, *Corros. Sci.*, 52 (2010) 314.
39. H. Ashassi-Sorkhabi, N. Ghalebsaz-Jeddi, F. Hasemzadeh, H. Jahani, *Electrochim. Acta,* 51 (2006) 3848.
40. P. Li, J. Y. Lin, K. L. Tan, J. Y. Lee, *Electrochim. Acta,* 42 (1997) 605.
41. D. A. Lopez, S. N. Simison, S. R. de Sanchez, *Electrochim. Acta,* 48 (2003) 845.
42. M. Yadav, D. Behera, S. Kumar, *Surf. Interface Anal.*, 46 (2014) 640.
43. O. E. Barcia, O. R. Mattos, *Electrochim. Acta*, 35 (1990) 1601.
44. D. Q. Zhang, X. M. He, Q. R. Cai, L. X Gao, G. S. Kim, *J. Appl. Electrochem.,* 39 (2009) 1193.
45. S. Varvara, R. Bostan, L. Gaina, L. M. Muresan, *Mater. Corros.,* 65 (2014) 1202.
46. D. Asefi, M. Arami, N. M. Mahmoodi, *Corros. Sci.*, 52 (2010) 794.
47. A. V. Benedetti, P. T. A. Sumodjo, K. Nobe, M. G. Proud, *Electrochim. Acta,* 40 (1995) 2657.
48. X. Wu, H. Ma, S. Chen, Z. Xu, A. Sui, *J. Electrochem. Soc.*, 146 (1999) 1847.
49. M. E. Folquer, S. B. Ribotta, S. G. Real, L. M. Gassa, *Corrosion,* 58 (2002) 240.
50. C. H. Hsu, F. Mansfeld, *Corrosion,* 57 (2001) 747.
51. B. Hirschorn, M. E. Orazem, B. Tribollet, V. Vivier, I. Frateur, M. Musiani, *Electrochim. Acta,* 55 (2010) 6218.
52. M. L. Zheludkevich, K. A. Yasakau, S. K. Poznyak, M. G. S. Ferreira, *Corros. Sci.*, 47 (2005) 3368.
53. S. Murlidharan, K. L. N. Phani, S. Pitchumani, S. Ravichandran, *J. Electrochem. Soc.*, 142 (1995) 1478.
54. S. M. A. Hosseini, A. Azimi, *Corros. Sci.*, 52 (2010) 2793.
55. E. E. Oguize, *Corros. Sci.* 50 (2008) 2993.
56. I. A. Ammar, F. M. El Khorafi, *Werkst. Korros.*, 24 (1973) 702.
57. E. S. Ivanov, *Inhibitors for Metal Corrosion in Acid Media*, Metallurgy, Moscow (1986)
58. F. Bentiss, M. Lebrini, M. Langrenee, *Corros. Sci.*, 47 (2005) 2915.
59. T. Szauer, A. Brandt, *Electrochim. Acta,* 26 (1981) 1209.
60. E. F. El Sherbini, *Mat. Chem. Phys.*, 60 (1999) 286.
61. N. M. Guan, L. Xueming, L. Fei, *Mater. Chem. Phys.*, 86 (2004) 59.

62. D. B. Hmamou, R. Salghi, A. Zarrouk, H. Zarrok, B. Hammouti, S. S. Al-Deyab, A. El Assyry, N. Benchat, M. Bouachrine, *Int. J. Electrochem. Sci*., 8 (2013) 11526.
63. S. Martinez, I. Stern, *Appl. Surf. Sci*., 199 (2002) 83.
64. J. O. M. Bockris, D. A. J. Swinkels, *J. Electrochem. Soc*., 111 (1964) 736.
65. E. A. Noor, A. H. Al-Moubaraki, *Mater. Chem. Phys*., 110 (2008) 145.
66. S. M. A. Hosseini, M. Salari, M. Abaszadeh, *Z. Phys. Chem*., 223 (2009) 769.
67. R. Solmaza, G. Kardas, M. Culha, B. Yazici, M. Erbil, *Electrochim. Acta,* 53 (2008) 5941.
68. M. Lebrini, M. Lagrenée, H. Vezin, L. Gengember, F. Bentiss, *Corros. Sci*., 47 (2005) 485.
69. F. Bentiss, M. Traisnel, M. Lagrenée, *Corros. Sci*., 42 (2000) 127.
70. W. Durnie, R. D. Marco, A. Jefferson, B. Kinsella, *J. Electrochem. Soc*., 146 (1999) 1751.
71. I. Ahamad, R. Prasad, M. A. Quraishi, *Corros. Sci*., 52 (2010) 1472.
72. S. Deng, X. Li, X. Xie, *Corros. Sci*., 80 (2014) 276.
73. B. Ateya, B. El-Anadauli, F. El Nizamy, *Corros. Sci*., 24 (1984) 509.